Available online at www.sciencedirect.com

ScienceDirect

Procedia Structural Integrity 28 (2020) 440–445

Structural Integrity Procedia

www.elsevier.com/locate/procedia

1st Virtual European Conference on Fracture

Crack propagation in 3PB specimen made from welded joint

M. Aranđelović[a], S.A. Sedmak[a]*, Lj. Milović[b], A. Maksimović[c], Ž. Božić[d]

[a]*Innovation Centre of Faculty of Mechanical Engineering, Kraljice Marije 16, 11120 Belgrade, Serbia*
[b]*Faculty of Technology and Metallurgy, University of Belgrade, Karnegijeva 4, 11120 Belgrade, Serbia*
[c]*Innovation Centre of Faculty of Technology and Metallurgy, Karnegijeva 4, 11120 Belgrade, Serbia*
[d]*Faculty of Mechanical Engineering and Naval Architecture, University of Zagreb, Ivana Lučića 5, 10002 Zagreb, Croatia*

Abstract

Crack propagation in 3PB specimen has been investigated experimentally by using Digital Image Correlation (DIC) technique. For this purpose, specimens were taken from butt welded plates, made of P460NL1 micro-alloyed steel. Fatigue pre-crack of 3PB specimens was introduced in the weld metal. Specimens were then statically loaded and analyzed using digital image correlation software ARAMIS to assess strain fields and crack propagation paths. Bifurcation of cracks was noticed as the main characteristics of crack prop-agation in the analyzed case.

Keywords: Digital image correlation, Crack propagation, Welded joint, Crack bifurcation

1. Introduction

In the recent years, there is an increasing trend in use of digital image correlation method in determining of displacement and strain fields, as well as in measuring of fracture mechanics parameters [1, 2]. This method has a number of advantages, such as high accuracy and its non-contact nature, as well as some disadvantages, and presented in this

* Corresponding author
E-mail address: simon.sedmak@yahoo.com

10.1016/j.prostr.2020.10.051

paper, are the results obtained with it, for a notched specimen with a welded joint, subjected to three point bending. The digital image correlation system used for this experiment consisted of two cameras (for the purpose of a 3D analysis) and ARAMIS software (GOM, Braunschweig) and has been successfully applied for welded joints in last few years, [4-8].

Prior to three point bending, a tensile test was performed in order to determine the mechanical properties of the weld metal which were required for the purpose of determining the dimensions of the test specimen, as well as for introducing a fatigue crack. Mechanical prop-erties of the parent material were taken from previous work [3].

2. Materials and method

For this paper, a welded joint specimen was cut from a welded plate made of P460NL1 steel, wherein FILTUB 12M solid wire was used as the additional material. The specimen was notched, wherein the notch was made in the middle of the weld metal area. Fatigue pre-cracking of 3PB specimens was done on the hydraulic testing machine 1332 INSTRON-100 kN by introducing a fatigue crack in the weld metal region of the welded joint. The length of the initial crack was 3 mm, wherein the depth of the notch was 7 mm. The geometry and dimensions of the notched specimen are given in figure 1, along with the position and initial length of the fatigue crack.

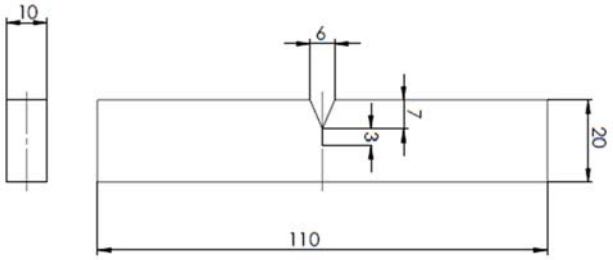

Figure 1. The dimensions of the test specimen, including the fatigue crack.

The mechanical properties of both materials, which were required for the fatigue crack and dimensioning of the specimen, are shown in table 1. It should be mentioned that the properties of the parent material were known from previous research, whereas the properties of the weld metal were determined based on a series of tensile tests, using load-displacement diagrams. The effective yield strength of the weld metal was determined according to ASTME 18-20 standard, as the mean value between the yield strength for plasticity of 0.2 and the ultimate tensile strength, wherein the average value for three specimens was adopted. The chemical composition of the materials used is given in table 2, [3].

Table 1. Mechanical characteristics of parent and additional materials

Material	Yield stress (MPa)	Ultimate tensile strength (MPa)	Elongation (%)
P460NL1	460	620	19
FILTUB 12M	535	580	24

Table 2. Chemical composition of parent and filler materials

Material	C	Si	Mn	P	S	Al
P460NL1	≤ 0.20	0.40	1.45	≤ 0.02	≤ 0.02	≥ 0.020
FILTUB 12M	0.05	0.55	1.40	-	-	-

Digital image correlation was performed during the three point bending test. The DIC system records the surface structure of a non-deformed measured object in form of series of digital images, and then assigns coordinates to every

pixel in the image, [1, 2]. Specimens are pre-pared for recording by applying a layer of white paint to the surface, which is then covered by finely dispersed black paint, creating a mesh of dots, which serve as pixels. Additional images were made while the load was being applied and were then compared with the initial (undeformed) one and in this way, displacement and strain of characteristic points or parts of the specimen were calculated [1, 2]. These images also provided insight into the propagation of the initial fatigue crack. In addition to the cameras, two light sources were used, in order to obtain better quality images. However, calculations are limited to local level displacements that are tangent to the surface, and the strain in the direction perpendicular to it is considered constant, which represents a disadvantage of the method, and should be taken into account. In addition, the cameras must be calibrated before recording, to ensure that the obtained results are as accurate as possible.

The experimental setup used for tensile and three point bending tests is shown in figure 2, along with the specimen after it was prepared for digital imaging, and the tensile test ma-chine (1332 INSTRON-100 kN). A detailed view of the prepared test specimen can be seen in figure 3.

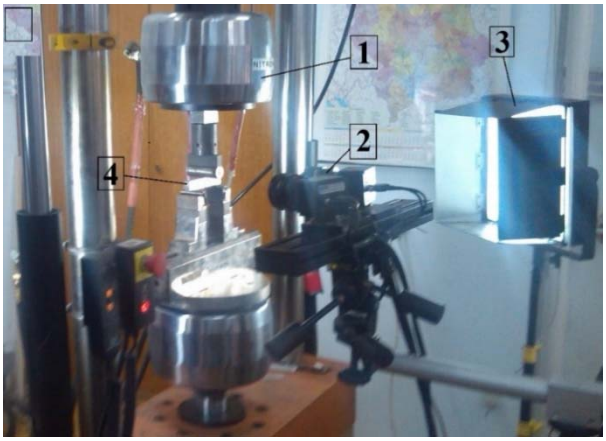

Figure 2. The experimental setup - 1) 1332 INSTRON - 100 kN test machine, 2) Cameras, 3) Light source 4) The specimen

Figure 3. The prepared specimen, prior to loading

Digital image correlation was performed in 49 stages (including the initial stage), for various load levels, including the point at which maximum force was reached, as well as the points where it started decreasing. The values of force for each stage are shown in the table below. Stage 10 was omitted due an error during the recording, which did not affect the other results. The force-displacement diagram is shown in Fig. 4.

Table 3. Force values at digital image recording stages

Stage	Force (N)	Stage	Force (N)	Stage	Force (N)	Stage	Force (N)	Stage	Force (N)
0	0	11	7870	21	9200	31	9400	41	8500
1	965	12	8010	22	9310	32	9320	42	8400
2	1880	13	8210	23	9350	33	9250	43	8300
3	3030	14	8370	24	9400	34	9150	44	8170
4	4370	15	8505	25	9450	35	9100	45	8100
5	4850	16	8705	26	9500	36	9000	46	8000
6	5570	17	8850	27	9550	37	8900	47	7800
7	6400	18	8900	28	9550	38	8800	48	7600
8	6570	19	9000	29	9500	39	8700	49	7400
9	6920	20	9100	30	9460	40	8600		

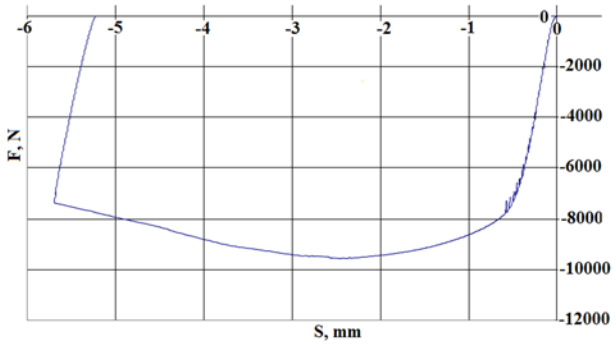

Figure 4. Force displacement diagram for the specimen

3. Results

Results for strain distribution obtained by digital image correlation are presented in Figs. 5-8., while more detailed view of one of the stages (where maximum plastic strain has occurred) is shown in figure 9, along with the geometry of the propagated crack.

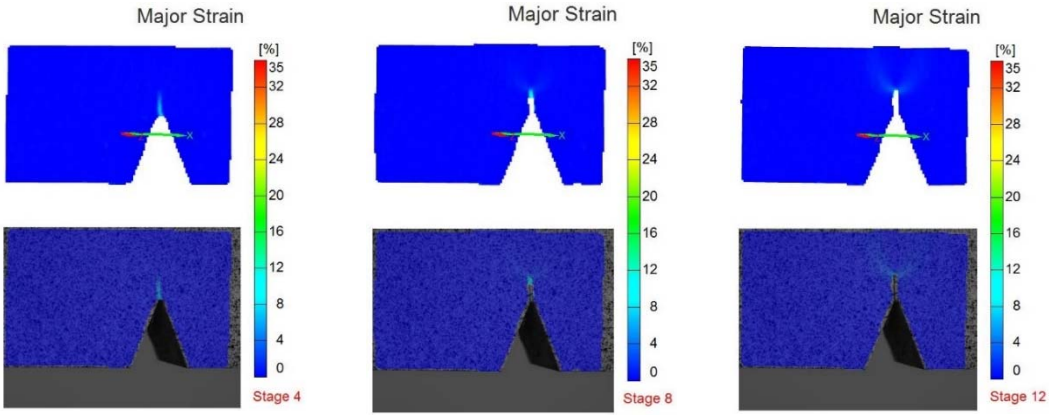

Figure 5. Strain results obtained by DIC (Stages 4, 8, 12)

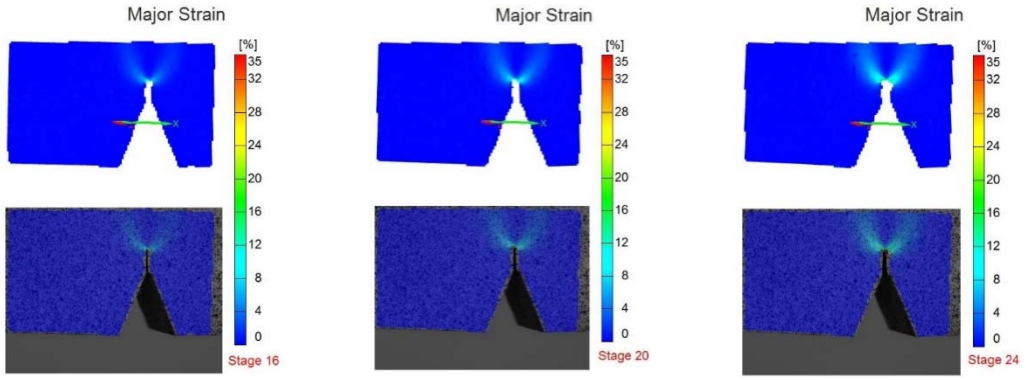

Figure 6. Strain results obtained by DIC (Stages 16, 20, 24)

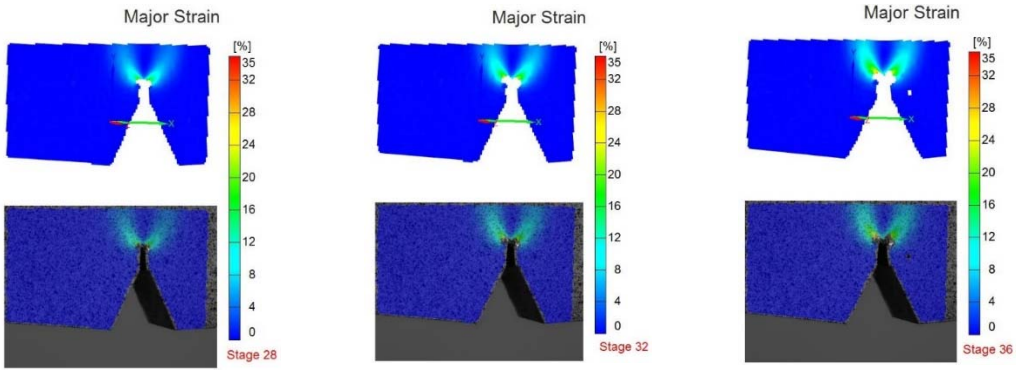

Figure 7. Strain results obtained by DIC (Stages 28, 32, 36)

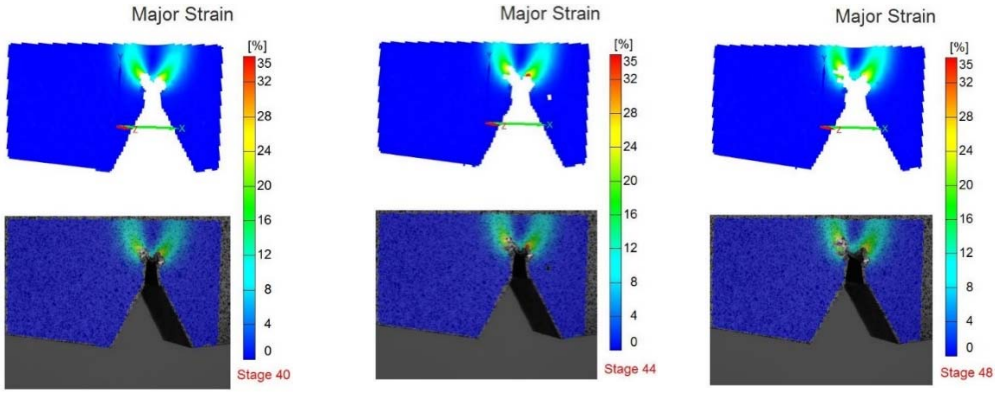

Figure 8. Strain results obtained by DIC (Stages 40, 44, 48)

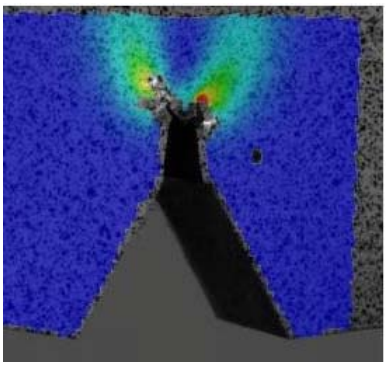

Figure 9. A detailed view of strain distribution at Stage 44.

4. Discussion

From the images shown in the previous figures, the crack propagation can be clearly seen. The crack itself can be observed at the beginning of the loading, denoted by a slightly different color compared to the surrounding area in the early stages (fig. 4). As expected, the strain was concentrated near the crack tip, as indicated in the later stages, as the crack propagation takes place (figs. 5-7). As can be seen from table 3, Stage 28 corresponds to the maximum force of 9550 N. The homogeneous appearance of the strain field in the images (homogeneous in this case refers to the fact, that there are barely any empty points, such as the one in Stages 36 and 44). This suggests that the specimen has been exceptionally well prepared for DIC optical measuring. This, in combination with camera calibration which was performed prior to the testing, resulted in the obtaining of accurate and representative results.

Strain which corresponded to the maximum force was determined to be around 15%, which corresponded to the value from the load-displacement diagram obtained by the experiment (vertical displacement at maximum force was 2.55 mm, i.e. the strain was ~13% since the specimen height was 20 mm). Maximum strain obtained by DIC was 35%, wherein the experimentally measured strain was around 29% (corresponding to a force of 7400 N), hence there was a bigger difference in this case, compared to the values at maximum force (of ~18% compared to 13% for maximum force).

5. Conclusions

Based on the results obtained by both digital image correlation and presented in this paper, it can be concluded that DIC can be used to measure the strain distribution of welded joint specimens subjected to three point bending load, with a satisfying level of accuracy. It should be pointed out, however, that this accuracy decreases after the maximum force is reached, and the load starts to decrease. The method also provided detailed insight into the propagation of the crack, by recording its various stages, and providing a clear digital representation, from the initial to the final stage.

Additionally, it can be concluded that the preparation of the specimen itself, along with proper calibration of the cameras, represent important factors in the accuracy and quality of the obtained results. These factors should always be taken into account in order to avoid possible errors during optical measuring.

The next step in this research should involve the development of a numerical model in order to compare different methods of determining the strain field in a three point bending specimen, along with their corresponding crack propagations.

6. Acknowledgements

The authors of this paper acknowledge the support from Serbian Ministry of Education, Science and Technological Development.

References

[1] McNeill SR, Peters WH, Sutton, MA. Estimation of stress intensity factor by digital image correlation, Engineering Fracture Mechanics, Vol. 28, No. 1, 1987.
[2] Nenad Gubeljak, Application of stereometric measurement on structural integrity, Structural Integrity and Life (2006), Vol.6, No. 1-2, 65-74
[3] Jovičić, R., Sedmak, S., Tatić, U., Lukić, U., Walid, M.: Stress state around the imperfections in welded joints, Integritet i Vek Konstrukcija, Vol. 15, No. 1, 2015
[4] Đordjević B., Tatić U., Vučetić F., Milošević M., Sedmak S., Effect of DIC equipment calibration on deformation measuring errors, Second International Conference on Modern Methods of Testing and Evaluation in Science, Belgrade (Serbia), 14-15.12.2015
[5] Lozanović, j., Gubeljak, N., Sedmak, A., „Measurement of Strain Using Stereometry“, Technical Ga-zette, No 4, Vol. 16, p. 93-99, 2009
[6] Nenad Mitrovic, Milos Milosevic, Aleksandar Sedmak, Aleksandar Petrovic, Radica Prokic-Cvetkovic Application and Mode of Operation of Non-Contact Stereometric Measuring System of Biomaterials, FME Transactions (2011) 39, 55-60
[7] Milosevic Milos, Mitrovic Nenad, Jovicic Radomir, Sedmak Aleksandar, Maneski Tasko, Petrovic Ale-ksandar, Aburuga Tarek, Measurement of Local Tensile Properties of Welded Joint Using Digital Image Correlation Method, CHEMICKE LISTY 2012 106 ():S485-S488
[8] A. Sedmak, M. Milošević, N. Mitrović, A. Petrović, T. Maneski, Digital Image Correlation in Experi-mental Mechanical Analysis, Structural Integrity and Life (2012), Vol. 12, No. 1, 39-42